

Deep-etch EM reveals that the early poxvirus envelope is a single membrane bilayer stabilized by a geodetic “honeycomb” surface coat

John Heuser

Department of Cell Biology, Washington University School of Medicine, St. Louis, MO 63110

Three-dimensional “deep-etch” electron microscopy (DEEM) resolves a longstanding controversy concerning poxvirus morphogenesis. By avoiding fixative-induced membrane distortions that confounded earlier studies, DEEM shows that the primary poxvirus envelope is a single membrane bilayer coated on its external surface by a continuous honeycomb lattice. Freeze fracture of quick-frozen poxvirus-infected cells further shows that there is only one fracture plane through this primary envelope, confirming that it consists of a single lipid bilayer. DEEM also illustrates that the honeycomb coating on this

envelope is completely replaced by a different paracrystalline coat as the poxvirus matures. Correlative thin section images of infected cells freeze substituted after quick-freezing, plus DEEM imaging of Tokuyasu-type cryo-thin sections of infected cells (a new application introduced here) all indicate that the honeycomb network on immature poxvirus virions is sufficiently continuous and organized, and tightly associated with the envelope throughout development, to explain how its single lipid bilayer could remain stable in the cytoplasm even before it closes into a complete sphere.

Introduction

One of the triumphs of early EM was the discovery that poxviruses package their genetic material into membranous spheres that form deep in the cytoplasm of infected cells, rather than by budding from the cells as do most other enveloped viruses (Wyckoff, 1951; 1953; Melnick et al., 1952). More marvelous still was the ensuing discovery that the spherical poxvirus envelopes form progressively by expansion of crescent-shaped precursors that display the same curvature as the final spheres, but start off incomplete and open to the cytoplasm (Bang, 1950; Gaylord and Melnick, 1953; Bernhard et al., 1954; Morgan et al., 1954, 1955). This very unusual form of membrane biogenesis has turned out to be quite novel, although it is seen in modified form in many of the large icosahedral DNA viruses that also form in the cytoplasm of infected cells (Smith, 1958; Breese and Deboer, 1966; Yule and Lee, 1973; Nunes et al., 1975; Mathieson and Lee, 1981; Meints et al., 1984, 1986; Brookes et al., 1998; Cobbold et al., 2000; Iyer et al., 2001; Van Etten et al., 2002; Stasiak et al., 2003). Certainly, no host-cell membranes have ever shown this pattern of biogenesis.

Even more intriguing is the fact that according to most electron microscopists, including all the original observers of

poxvirus formation and many microscopists still working today, the composition of the growing crescents and the final spheres is a single membrane bilayer (Dales and Siminovitch, 1961; Dales, 1963; Patrizi and Middelkamp, 1968; Dales and Mosbach, 1968; Pogo and Dales, 1969, 1971; Harford et al., 1972; Tripier et al., 1973; Morgan, 1976). This defies the common wisdom that all biological membranes form closed compartments, and must do so because a single membrane would expose a ragged, hydrophobic edge to the cytoplasm, which presumably would be intrinsically unstable.

Faced with this apparent dilemma, several studies of poxvirus morphogenesis sought data and EM images that would show that the poxvirus crescents and spheres are actually composed of two closely opposed membrane bilayers, as would result from complete collapse of the lumen of a closed compartment (Sodeik et al., 1993; Krijnse-Locker et al., 1996; Ericsson et al., 1997; Salmons et al., 1997; Griffiths, Roos et al., 2001; Sodeik and Krijnse-Locker, 2002). Unfortunately, the EM images obtained to date that argue for this simpler two-membrane model have not been entirely convincing. Moreover, the deep-etch EM (DEEM) images presented in this report confirm the original conclusion that the initial poxvirus envelope is indeed a single lipid bilayer. These are derived primarily from “quick-freeze, deep-etch” replicas, but also from thin sections of infected cells that were also quick frozen rather than chemically fixed as is usually done.

Correspondence to J. Heuser: jheuser@cellbiology.wustl.edu

Abbreviations used in this paper: 3-D, three-dimensional; DEEM, deep-etch EM; IMV, intracellular mature virion; IV, immature virion.

The challenge thus remains of how to explain how such an individual membrane can be stable in the cell and how it can grow (Hollinshead et al., 1999; Husain and Moss, 2003). These questions are provisionally answered here by the additional finding that the poxvirus envelope is uniformly and tightly coated by a meshwork of protein that forms a confluent honeycomb lattice on its convex surface: a lattice with a fixed and constant radius of curvature. It has long been known that this envelope has on its external surface what have been termed “spikes” (Stern et al., 1977; Dales et al., 1978; Mohandas and Dales, 1995; Risco et al., 2002). However, not until en face images of this envelope could be obtained by DEEM was it possible to fully appreciate that these so-called spikes are in fact the edge views of a fully confluent, continuously interconnected honeycomb lattice. Thus, we can now appreciate how this special protein coat could effectively “template” and stabilize the single membrane of the nascent poxvirus.

Results

Cross fractures through viruses at all stages of development

Fig. 1 diagrams the stages of viral morphogenesis that will be depicted in the images presented here, and displays the names currently used for each stage. Freeze fractures or cryosections through viral factories in cells infected overnight (Fig. 2, A–C) reveal all stages of virion development, from short arcs or “crescents” that represent the earliest stages of IV development, to closed spheres that represent the completion of IV development, to more condensed brick-shaped profiles that represent the mature intracellular virions (IMVs). Fig. 2 (A and B) compares freeze etchings of unfixed MVA-infected avian cells versus aldehyde-fixed WR-infected mammalian cells. (No structural differences of any sort can be discerned between viruses grown in these two cell lines, or between these two strains of virus.) In contrast, Fig. 2 C presents a survey view of a Tokuyasu-type cryosection made from a pellet of aldehyde-fixed WR-infected mammalian cells, where the cryosection has been freeze dried and replicated rather than viewed in the usual way (Tokuyasu, 1973). This yields images of virogenesis that look almost indistinguishable from standard DEEM images (Fig. 2, compare A with C). The only noticeable difference is that the added steps needed to prepare for cryosectioning make the cytoplasm look even more coarse and “microtrabecular” than does aldehyde fixation alone (Heuser, 2002). (To appreciate the effect of aldehyde fixation per se, B can be compared with A in Fig. 2.)

In any case, all such views illustrate that cross fractures (or Tokuyasu cross cuts) of the outer envelope of immature vaccinia virions yield an unusually thick lamina compared with other cross fractured membranes. The IV envelope measures 15–20-nm thick rather than the usual 7–10 nm of a standard intracellular membrane, due to the fact that it bears discernable mass its external or convex surface (Fig. 3, A–C). However, this added mass does not appear to represent a second membrane, because it looks too discontinuous or “studded”. By comparison, Fig. 3 (D and E) illustrates that intracellular or-

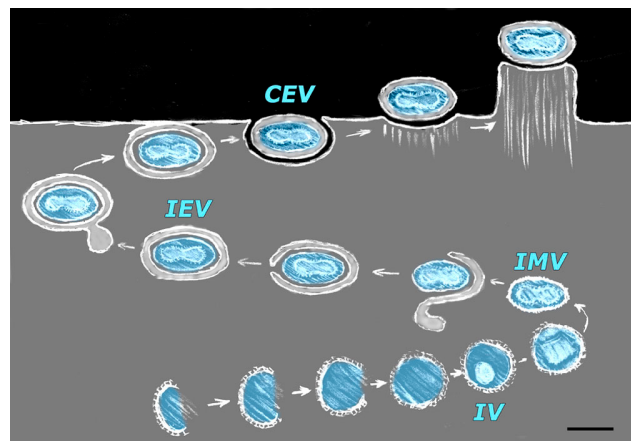


Figure 1. Stages of morphogenesis of vaccinia virus, the prototypical poxvirus, including the abbreviated names of each stage. Virogenesis begins with the formation (from crescent-shaped precursors) of a spherical immature virion (the “IV”). The core of the IV then condenses and differentiates to form a mature intracellular virion (IMV). The naked IMV is then enveloped by a collapsed cisterna of intracellular membrane (of unknown origin) to form an intracellular enveloped virion (the “IEV”). The IEV then behaves like a recycling endosome, moving along microtubules to the cell surface where it ultimately fuses with the plasma membrane to release an IEV derivative that is still wrapped in one of the two layers of its original envelope. Typically, this particle remains attached to the cell after discharge, thus is called a cell-associated enveloped virion or “CEV.” However, if and when it breaks free from the cell surface it is called an extracellular enveloped virion or “EEV” (not depicted). Some CEV’s on the cell surface provoke oriented actin polymerization inside the cell (“actin tail formation”), thereby elevating themselves on the tip of a blunt microvillus. This promotes their fusion with neighboring cells and the spread of infection. Bar, 0.3 μm.

ganelles known to be double membraned like mitochondria (Fig. 3 D) and even the host cell envelopes that secondarily engulf vaccinia virions as they mature (Fig. 3 E) invariably do display their double-membrane nature after freeze fracture. (Both panels D and E of Fig. 3 include cross fractured IVs in the same field, to further demonstrate this critical difference.) Likewise, comparable thin sections of quick-frozen and freeze-substituted cells (Fig. 4) confirm that the outer envelope of the vaccinia virion can be resolved into a ~7-nm electron-lucent central layer sandwiched between two electron-dense layers, the outer one looking much thicker and spiky looking on IVs and looking irregular on IMVs. Again, this envelope looks very different from cytoplasmic double membranes like mitochondria, as illustrated in the bottom, magnified panels of Fig. 4.

Cross fractures of viral cores

Cross fractures also yield images of the cores in all the developmental forms of vaccinia virions, which vary widely in consistency, from only a little denser than the surrounding viroplasm in IVs, to very dense and compacted in IMVs, with all degrees of condensation in between (Fig. 2, A–C). Most notable is the distinct discontinuity observed between the uniformly granular interior of the IV and the distinctly laminated interior of the IMV, where a second complete layer can be discerned inside the outer envelope. This second layer is particularly apparent in Tokuyasu cryosections (Fig. 2 C), simply because an ultramicrotome with a diamond knife is more

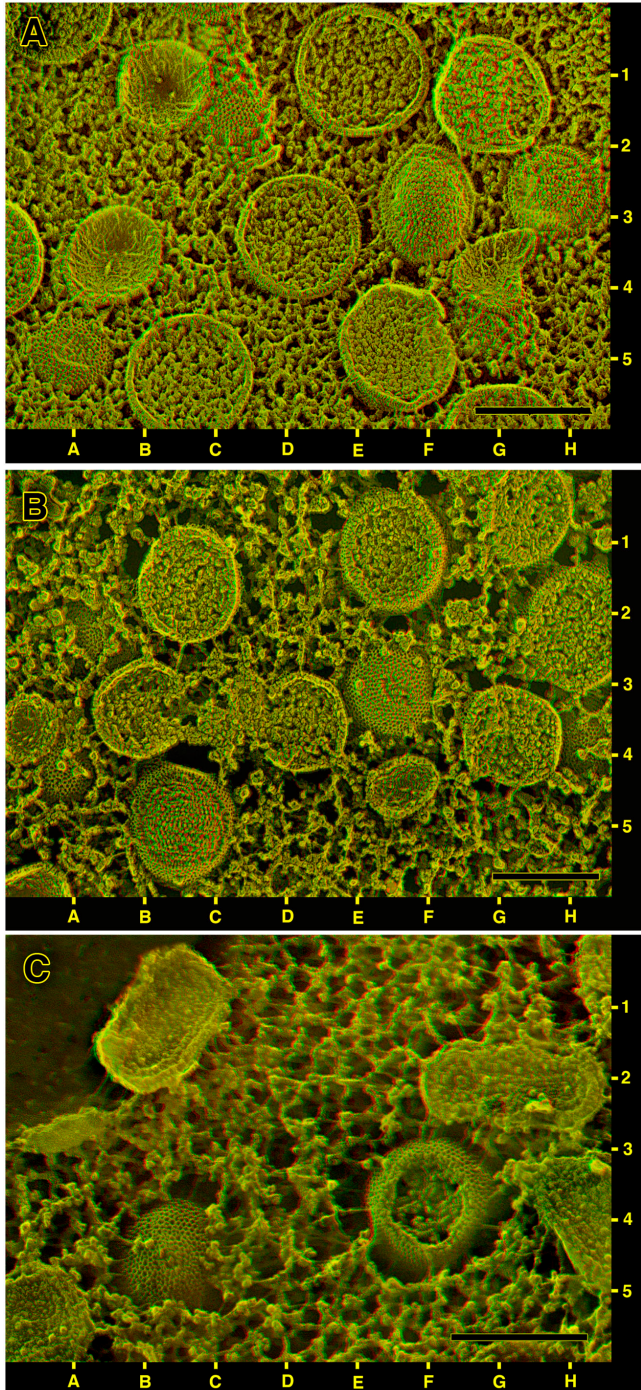


Figure 2. Survey views of viral factories in cells infected overnight and then prepared by different protocols for DEEM. (A) QT6 quail cells infected with the MVA strain of vaccinia virus and quick-frozen alive, without any chemical fixation or other pretreatment. Only immature virions (IVs) are present in this field, but they look different depending on the plane of fracture. Cleanly cross fractured IVs, the large circles with granular interiors, are seen at 1E, 3D, and 5C. Freeze-fractured IVs that have been “scalped” are seen at 3F and 3H (and one with a small “scalping” at 5A). Fractured IVs that have been largely avulsed, leaving only cup-shaped membrane remnants, are seen at 1B, 3B, and 4G. The cross fractured IVs at 1G and 5F show some compaction of their cores and hints of icosahedral shape, indications of incipient maturation. Just peeking out from the uniformly granular cytoplasm at 1C and 4G are two whole unfractured IVs showing surface honeycombs. (B) BS-C-40 cells infected with the WR strain of vaccinia virus and then strongly fixed with glutaraldehyde before freezing. Such fixation coagulates the cytoplasm and causes it to with-

successful at “cross cutting” IMVs than is the standard freeze-fracture microtome. Nevertheless, this second layer is still clearly visible in clean freeze fractures of IMVs in totally unfixed cells (Fig. 5, top). Thin sections of freeze-substituted cells confirm that this inner lamina is the so-called “palisade” layer of the IMV, generally considered to be the surface of the virion “core” proper (Fig. 4; Easterbrook, 1966; Muller and Williamson, 1987; Dubochet et al., 1994). Thin sections of quick-frozen IMVs such as Fig. 4 also match closely all earlier images of chemically fixed virions (Dales and Siminovitch, 1961; Dales, 1963; Morgan, 1976; Muller and Williamson, 1987), showing in suitable orientations two slightly denser “lateral bodies” in the viral “periplasm,” in between the palisade layer of the core and the outer envelope of the virion. Although these lateral bodies are only barely discernible in the freeze-fracture images, on the basis of a slight difference in physical consistency (Fig. 5, top), still their existence can be convincingly inferred from the overall shapes of unfixed IMVs, which in suitable orientations appear embossed on their surfaces by these lateral bodies (Fig. 6, bottom). Not depicted are corroborative DEEM images we have obtained of purified vaccinia virus cores generated by detergent extraction of isolated IMVs, in which case the lateral bodies are retained on the surface of the cores and thus are fully exposed and immediately apparent. They are clearly not an artifact, as one group once claimed (Dubochet et al., 1994).

Surface views of intracellular viruses’ “honeycomb coats”

Unique to the deep-etch technique is its ability to display the surface features of intracellular membranes and membrane coatings. Such features are essentially invisible in traditional thin sections and cannot even be retrieved EM tomography, due to the chronic problem of the “missing wedge” in all tomographic datasets (Heuser, 2001). In the case of vaccinia virus, this unique capability of DEEM displays to advantage the standard features seen on the surfaces of IMVs (Fig. 6, B and C). These have been recognized for decades (Dales, 1962; Noyes, 1962a,b; Harris and Westwood, 1964; Nermut, 1972; Muller and Williamson, 1987; Ikoma et al., 1992). However, DEEM reveals in addition a wholly new and unexpected feature of the surface of the IV. Namely, it is not covered by a discontinuous

draw from all the IVs in the field, thereby providing more expansive views of their honeycombed surfaces (at 3F, 2B, 4A, and 4H). Freeze-fracture views look the same as in Fig. 2 A however, showing both convex “scalped” IVs (at 5B) and concave avulsed IVs (at 3A, 4F). Also present in this field (not depicted in Fig. 2 A) are two incomplete crescent-shaped IV precursors partially filled with viroplasm (at 3B and 4D). (C) Tokuyasu-type cryosection that was freeze dried and replicated rather than viewed in the traditional manner. The preparation for cryosectioning causes even more severe coagulation of the cytoplasm and more exposure of the IV surface honeycomb (at 5B and 4F). Also present in this field are four cross cut intracellular mature viruses (IMVs) at 1B, 2G, 4H, and 5A. The one at 2G is optimally oriented for seeing its internal core. Note that in such cryosections, “scalped” IVs like the one at 4F do not retain any fracture faces. These must break down during cryosectioning and/or thawing. Instead, scalped IVs in such cryosections show complete breaks into their interiors. Bars, 0.3 μm.

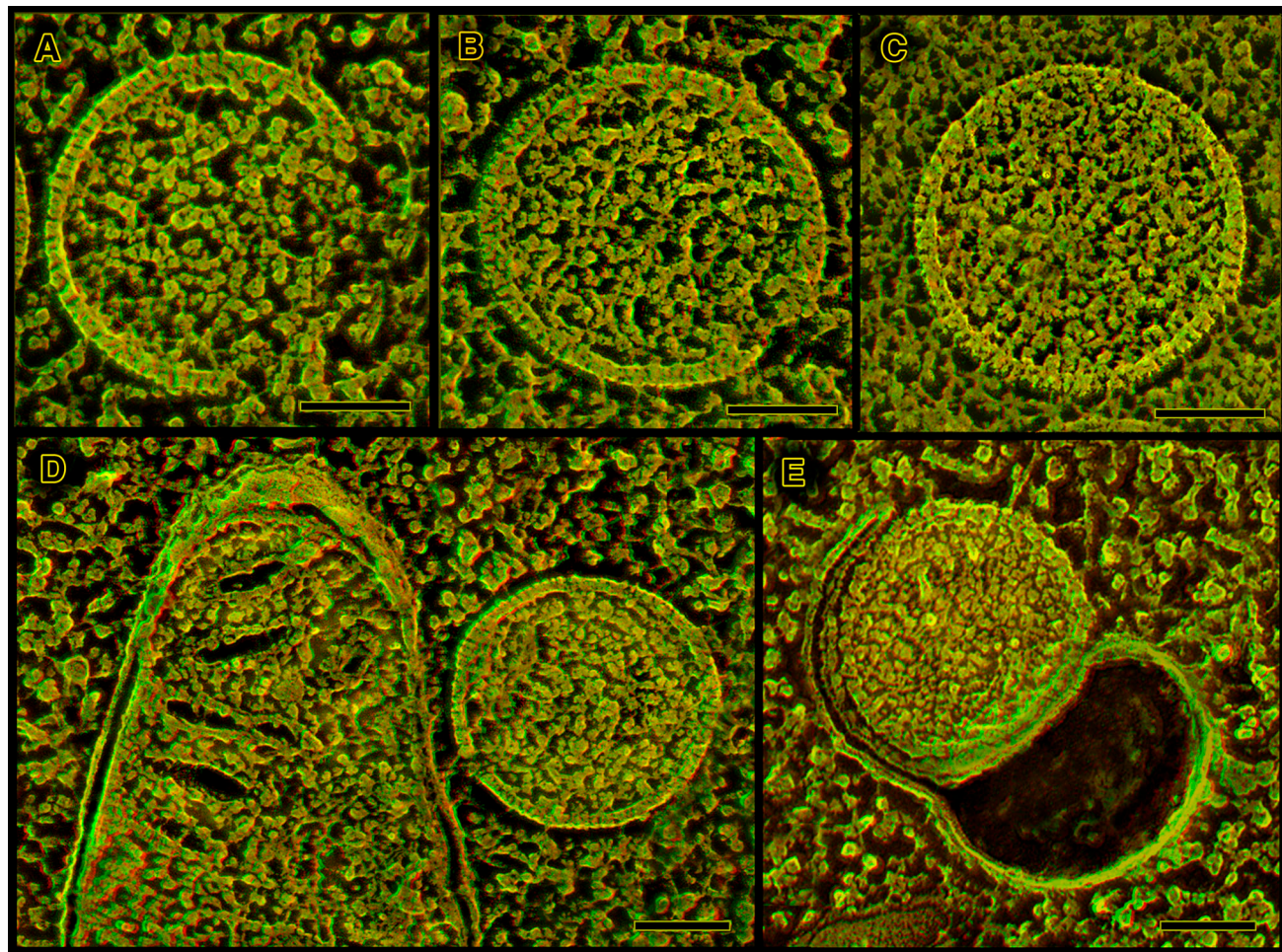


Figure 3. Higher magnifications of cross fractured vaccinia IVs from completely unfixed cells like that depicted in Fig. 2 A. Their surrounding envelopes are invariably $>2\times$ thicker than the usual membrane bilayer and are punctuated on their convex surfaces with “pegs” or particles that are presumably the deep-etch equivalent of the “spikes” seen in traditional thin-section views of IVs. A and B display incomplete IV-crescents at different stages of formation. In contrast to their appearance in cells prepared by chemical fixation and dehydration, none of the crescents in quick-frozen cells show any attachments to other cellular membranes, at all. Occasionally their free edges appear to contact nondescript 15–20-nm globules, but otherwise they appear to end completely blindly, as shown here. C illustrates the completed IV sphere. D and E show that other organelles in infected cells that do possess double-thickness envelopes. D shows a mitochondrion whereas E shows a developing vaccinia IEV, where a dark, empty-looking host cell organelle appears to be extending a thin cisterna around the developing virion. In both cases, these organelles cross fracture in a way that clearly shows their construction: two distinct membranes of normal thickness separated by a narrow gap, unlike the IV membrane which is thicker but does not look like two closely opposed membranes. Bars, 0.1 μm .

layer of spikes, as appeared in earlier thin sections (Stern et al., 1977; Dales et al., 1978; Mohandas and Dales, 1995; Risco et al., 2002), but is in fact covered by a confluent honeycomb lattice. This lattice is visible even in the low magnification survey views of Fig. 2 (A–C), but is seen to better advantage at higher magnification as shown in Fig. 7.

No doubt, this lattice appeared spiky in earlier thin sections because it is so tightly applied to the exterior of the virus, and because at certain viewing angles its facets align and reinforce in an EM image. The only previous hints that this coating could possibly be a honeycomb lattice came from a couple of glancing thin section images of it published earlier (Mohandas and Dales, 1995; Risco et al., 2002), plus an obscure freeze-etching paper published by Hung et al. (1980), who caught a glimpse of what they described in the legend to their Fig. 1 as “some tiny crystalline structures....with a hexamer-like subunit arrangement.” We can now appreciate that these authors were

correct in interpreting these tiny hexamers as being glimpses of something “on the presumptive surface of a virus particle” (Hung et al., 1980). Current DEEM now shows clearly the full expanse of this impressive honeycomb lattice, which is seen equally well on unfixed IVs of MVA (Fig. 2 A and Fig. 7), as it is on aldehyde-fixed freeze fractures of WR (Fig. 2 B) or Tokuyasu-type cryosections of WR (Fig. 2 C). As usual, it is barely visible in thin sections of freeze-substituted material because it is only 10-nm thick, and thus is obscured by the 100–200-nm total thickness of the plastic section (Fig. 4).

Close examination of the vaccinia viruses’ surface honeycomb reveals that it is remarkably similar in construction to the honeycomb lattice that surrounds clathrin-coated vesicles, except that it is much more compact and multifaceted (Fig. 7). The number of facets in the vaccinia virion lattice is at least an order of magnitude greater than in clathrin-coated pits (the facets being just 40% the size of those in the clathrin lattice and

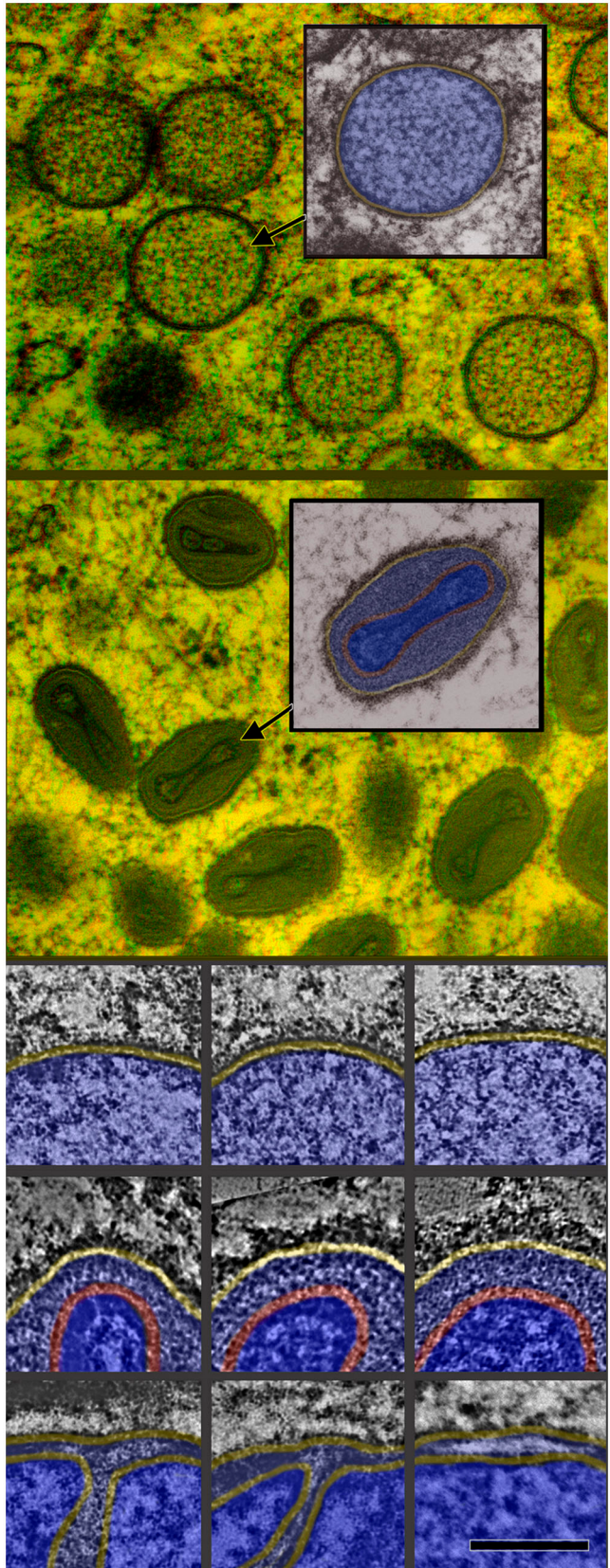


Figure 4. Semithin plastic sections of cells infected overnight with MVA, then quick-frozen from life and freeze substituted. Top (3-D): Survey view of a field of IVs with one selected and color coded with membrane in yellow and core in blue. Second (3-D): Survey view of a field of IMVs with one selected and color coded with membrane in yellow and core in two shades of blue, separated by its palisade layer in red. (Top triptych, not 3-D)

the virion being more than two times the diameter of a coated vesicle or four times its surface area). Additionally, the vaccinia virion lattice is somewhat less regular than the clathrin lattice and less obedient of classical geodesic construction principles (e.g., the standard alteration of five- and six-sided facets, etc.; Buckminster-Fuller and Applewhite, 1975). That is, many more lattice-discontinuities are seen in the vaccinia virion honeycomb than in the clathrin lattice. The bottom panels in Fig. 7 illustrate that its honeycomb displays many more pentagon/hexagon dislocations that were ever discerned in growing clathrin-coated pits (Heuser, 1980, 1989; Steer and Heuser, 1991). Because all such honeycombs are built out of trimeric elements located at each vertex of the lattice, we can conclude that there must be more variability in the lateral interactions of the vaccinia virion trimers than in the interactions of clathrin triskelia. This presumably reflects the simple fact that the vaccinia virion lattice is so compact compared with clathrin, so the lateral interactions of the trimers in its lattice must be much more limited in extent than the complicated interactions that exist amongst the very extended 645-kD “triskelia” of the clathrin lattice (Heuser and Kirchhausen, 1985; Kirchhausen et al., 1986; Heuser et al., 1987; Heuser and Keen, 1988; Nathke et al., 1992; Prasad et al., 1994).

Despite these dislocations, the nascent poxvirus honeycomb coat must be sufficiently confluent and interlocked to be relatively rigid, because even the smallest pieces of it (on the surface of the shortest arcs of developing IVs; compare Fig. 3, top) already display a remarkably fixed radius of curvature ($R = 0.14 \pm 0.02 \mu\text{m}$), which closely matches that of the complete IV sphere. (IVs are remarkably uniform in diameter at $D = 0.3 \pm 0.03 \mu\text{m}$.) Apparently, this degree of curvature is built into the honeycomb network as it associates with the virion membrane. (In a subsequent report, we will show that overexpression of the pure coat protein in cells, in the absence of membrane association, forms instead totally flat honeycombs with no lattice discontinuities or pentagons.) Other indications of the relative rigidity of the vaccinia virion lattice is that IVs do not swell when infected cells are swollen (or even burst) by exposure to distilled water (not depicted); nor do they collapse when cells are grossly shrunken by the 2M sucrose used to prepare Tokuyasu-cryosections (Fig. 2 C). (This fixed-curvature aspect of the poxvirus lattice again differs significantly from the honeycomb lattices of clathrin seen in cells. Due to the relatively extended nature of their component triskelia and the high degree of overlap of these triskelia, clathrin lattices display a wide range of curvatures and are capable of forming endocytic vesicles with a wide variety of sizes and shapes (Heuser, 1980, 1989; Heuser et al., 1987; Steer and Heuser, 1991; Nathke et al., 1992; Prasad et al., 1994).

Higher magnification of portions of IVs showing their single surrounding membrane (yellow) with hints of spikes on their external surfaces. (Middle triptych) Equally high magnifications of portions of IMVs showing the characteristic separation between their outer limiting membrane (yellow) and their palisade layer (red). (Bottom triptych) Portions of three freeze-substituted mitochondria at the same high magnification showing the characteristic thickness of their two membranes and the characteristic separation between them. Bar: (top 3-D views) $0.3 \mu\text{m}$; (tryptics) $0.1 \mu\text{m}$.

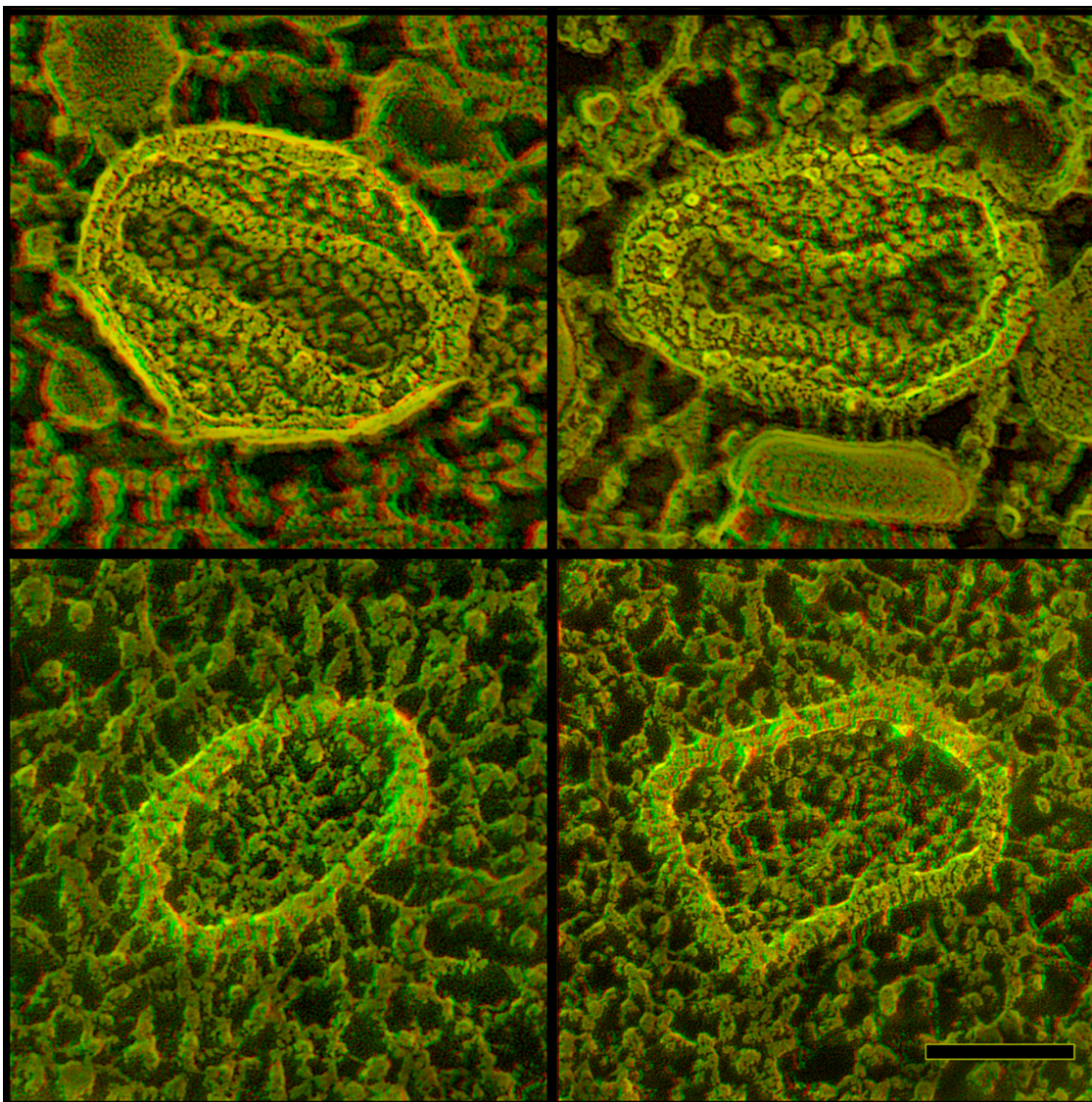


Figure 5. Direct comparison of the architecture and fracturing properties of the internal “palisade layer” around the cores of intact versus fused virions. (Top) Cross fractures through totally unfixed IMVs from cell like that in Fig. 2 A, showing a clear view of the internal “palisade layers” around their biconcave cores, and showing that these layers do not fracture like a biological lipid membrane. (Bottom) Crossfractures through viral cores recently released into the cytoplasm of a cell exposed to a whopping dose of vaccinia virions by “spinoculation” and quick frozen after only 5 min. The palisade layers surrounding these cores are still clearly discernible and look more or less intact. Nevertheless, even in this naked “exposed” condition in the cytoplasm, they do not freeze fracture like any membrane-containing structure. Instead, they invariably crossfracture like the palisade layers in the intact IMVs above, indicating that they are composed of nothing but protein (and polynucleotides). Bar, 0.1 μ m.

Surface views of the IMV

The honeycomb surface of IVs apparently completely disappears by the time the poxvirus matures into an IMV. Instead, intracellular IMVs appear more roughly textured or corrugated on their surfaces (Fig. 6 A). However, IMVs are extremely difficult to image *in situ* by DEEM, simply because the surrounding cytoplasm of the cell clings tenaciously to them and thus obscures their surfaces. This makes it all the more remarkable that the surfaces of IVs inside the cell are so easy to see, and their honeycombs appear so clean. Apparently, this is because the honeycomb repels cytoplasm from its surface. Fig. 6 B illustrates that comparably clean images of IMV surfaces can only be obtained by freeze-drying IMVs that have been released from CEVs during a natural cycle of

infection. These latter virions display a characteristic corrugated appearance, due to a close-packing on their surfaces of short “railroad tracks” composed of parallel rows of particles. On the vaccinia virions studied here, these railroad tracks run only short distances and intersect with each other in a haphazard pattern. They have only occasionally been glimpsed before (Medzon and Bauer, 1970; Nermut, 1972, Muller and Williamson, 1987). However, on certain other poxviruses such railroad tracks form beautiful helical arrays, as on Orf and Pseudocowpox viruses (Nagington and Horne, 1962; Horne and Wildy, 1963; Nagington et al., 1964, 1967; Mitchiner, 1969; Spehner et al., 2004.) Fig. 6 C illustrates for comparison an IMV released from a vaccinia-infected cell by the standard protocol of cell-rupture and trypsinization, after which

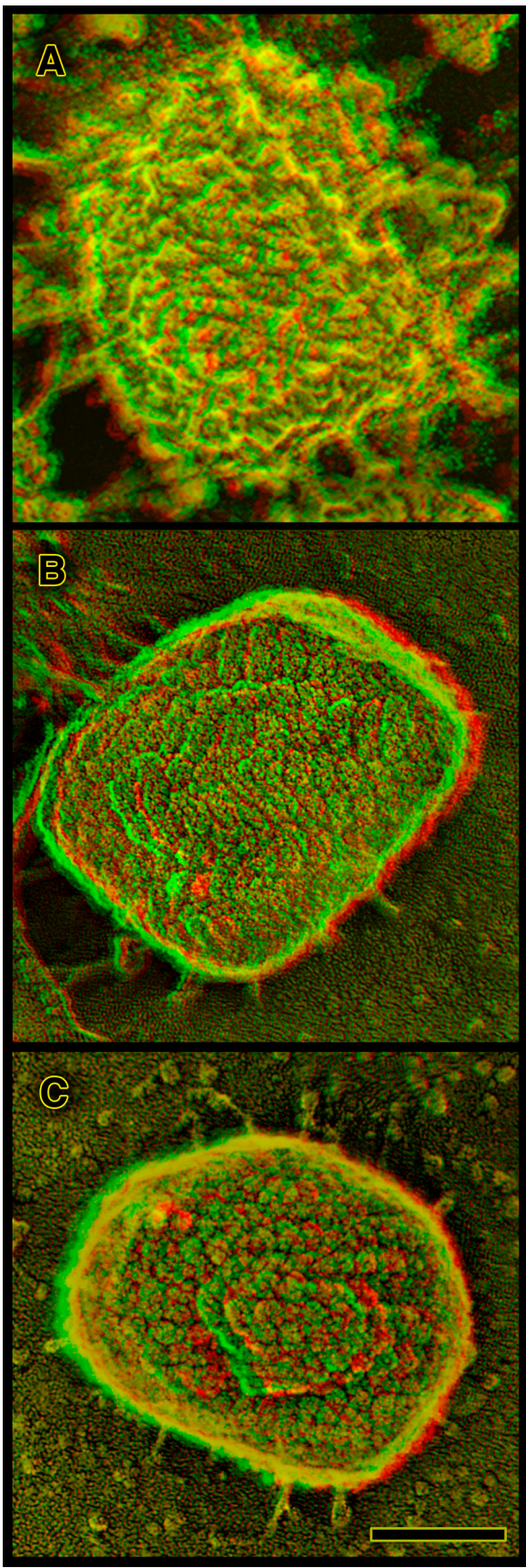


Figure 6. Three different sorts of views of the true surfaces of IMVs. (A) As seen inside whole cells during virogenesis; (B) after natural release as a CEV from an infected cell, followed by rupture of the CEV membrane

the organization of these railroad tracks becomes so haphazard and disorganized that they are barely recognizable. In this condition, the IMV has traditionally been described as having “mulberries” on its surface, not railroad tracks (Dales, 1962; Harris and Westwood, 1964; Muller and Williamson, 1987; Ikoma et al., 1992).

Freeze fracture of the envelopes of intracellular virions

The opportunity to image poxvirus surfaces greatly facilitates the interpretation of the underlying membrane “fracture faces” they yield. Such faces result from splitting the lipid bilayer roughly through its center during the freeze-fracturing procedure. With immature poxviruses, this invariably yields two roughly complementary sets of faces, convex and concave (Fig. 8 A). Convex faces are invariably found in regions that are obviously carved out of the surface-honeycomb of IVs (Fig. 8 B). In three-dimensional (3-D) views, it is clear that they represent 10–15-nm downward steps (presumably through the full thickness of the honeycomb and half of the lipid bilayer, as diagrammed in Fig. 8 A). In contrast, concave fracture faces look like isolated fragments of split membrane that are raised slightly above the surrounding cytoplasm (Fig. 8 C). Presumably, they sit upon the remaining segments of their external honeycomb (not visible because this honeycomb is now directly underneath the concave fracture face, again as diagrammed in Fig. 8 A).

Both IVs and IMVs fracture in the aforementioned manner, with only minor differences in the texture of the membrane faces thus exposed, as can be seen by comparing Fig. 8 (B and C) with the freeze fractures of IMVs shown in Fig. 9. It is worth pointing out here that the convex and concave fracture faces of vaccinia virions never look truly complementary, as they ought to if they are indeed the opposite halves of a single membranous structure. However, this disparity has always been seen in freeze fractures of biological membranes, and has long been interpreted as representing some degree of “plastic deformation” of internal membrane components during fracturing (despite the fact that fracturing is typically done at $>-100^{\circ}\text{C}$; Steere, 1957; Zingsheim, 1972; Fisher and Branton, 1974). Indeed, it has even been seen in the small handful of previous freeze-fracture studies of vaccinia virions that have been published (Medzon and Bauer, 1970; Easterbrook and Rozee, 1971; Hung et al., 1980; Risco et al., 2002). In the case of vaccinia virions, this incongruity is typically manifest as long

to expose a clean IMV inside; and (C) after douncing of infected cells and isolation of IMVs as is typically done to harvest virus for subsequent experimentation. Inside of the cell, cytoplasm clings tenaciously to the surface of IMVs, obscuring their surface. (This is apparent also in the survey of Fig. 2 C.) When harvested from cells, most of this obscuring material is removed (C), but the finer features of the IMV surface are degraded into what traditionally have been called “mulberries” (possibly due to the trypsinization and sonication typically used in such purification). When released in the course of a natural infection, and when the outer membranous envelope of the CEV ruptures to expose the IMV to neighboring cells, the IMV surface displays a clear-cut paracrystalline topology defined by parallel double rows of particles (B). Bar, 0.1 μm .

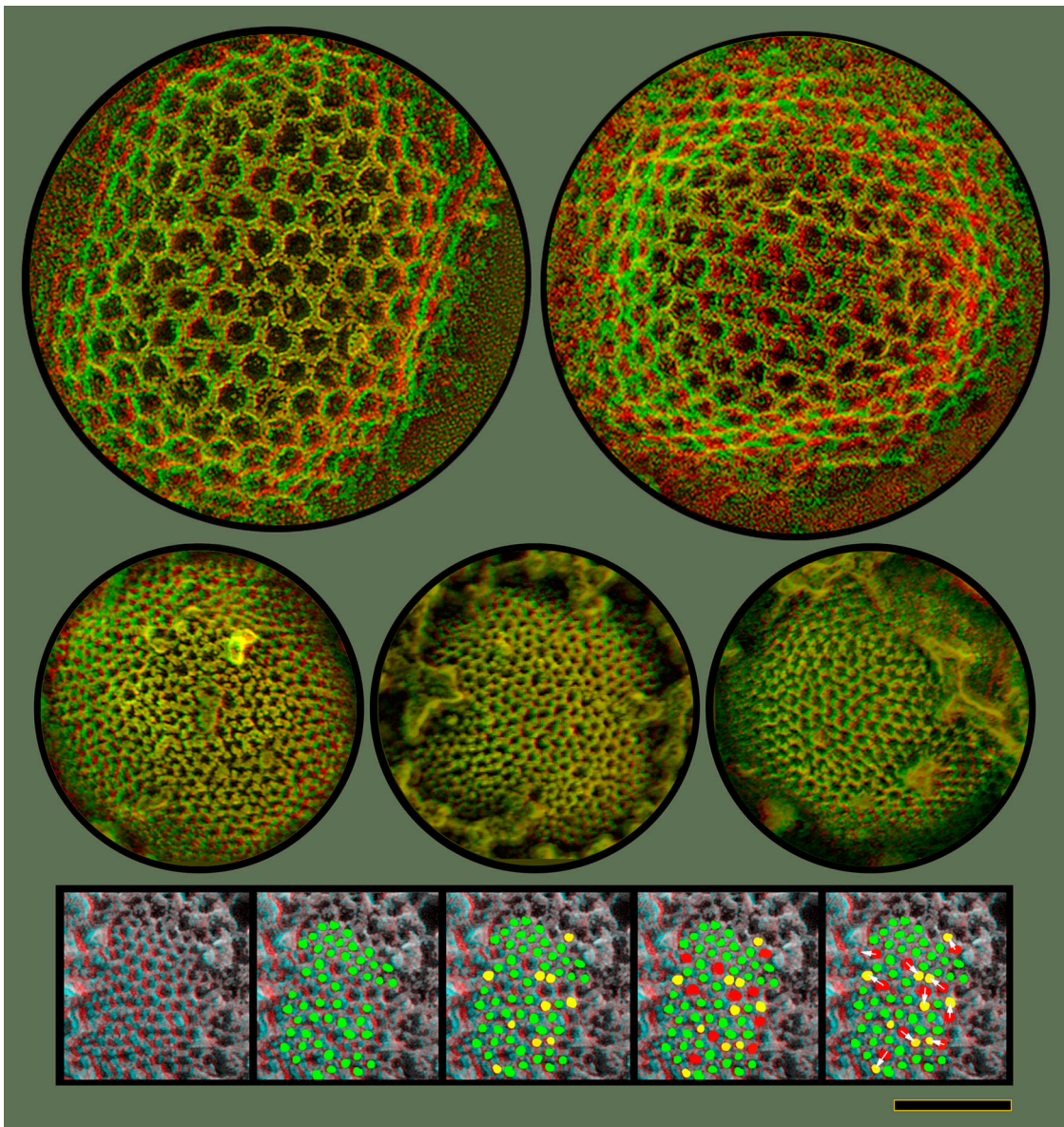


Figure 7. Direct comparison of clathrin lattices and the honeycomb lattices on IVs, shown at exactly the same magnification. The clathrin lattices (top) have lattice parameters $>2\times$ greater than the honeycombs on IVs (center). Expansive surface views of IVs are readily obtainable because surrounding cytoplasm appears to be repelled from them, in contradistinction to IMVs (Fig. 6 A). The protein lattice observed on the IV surface is clearly a geodetic honeycomb, and sometimes shows hints of overall icosahedral symmetry. However, its lattice dimensions are much smaller. Its vertex to vertex spacing is 7 ± 1 nm versus clathrin's 15 ± 1 nm. Moreover, the vaccinia lattice typically displays many more lattice-defects and irregularities. These irregularities invariably take the form of "pentamer/heptamer" dislocations, typical for all natural honeycomb lattices. Insets at the bottom illustrate this. Proceeding from the left, green dots indicate proper hexagonal facets and yellow dots indicate inserted pentagons. Only 12 of these pentagonal insertions would be needed in the whole lattice to make it a sphere, according to Crick and Watson's postulate (Crick and Watson, 1956; Caspar and Klug, 1962); but many more pentagons are visible in this relatively small portion of the IV surface. Finally, red dots indicate inserted heptagons and white arrows indicate how each of these heptagons can be matched with a pentagon immediately adjacent to it. Bar, 0.1 μ m.

threads that stretch out in random orientations on the concave fracture faces (Fig. 8 C), and dense granularity over the entire expanse of the convex faces (Fig. 8 B), neither of which is properly represented by complementary features on the opposite fracture face.

Not seen in any single instance, however, are any additional planes of fracture through the outer envelopes of either IVs or IMVs. In fact, no additional planes of fracture were ever described in any earlier freeze-fracture study of poxviruses (Medzon and Bauer, 1970; Easterbrook and Rozee, 1971; Ha-

segawa et al., 1974; Hung et al., 1980), although one study claimed to glimpse them but without adequate documentation (Risco et al., 2002). Such additional planes of fracture or "steppes" would definitely be expected if either IVs or IMVs contained of more than one membrane. Also not seen in any single instance were any direct physical connections between developing IV crescents and any adjacent host-cell membranes (Figs. 2–4). Indeed, DEEM confirms that poxvirus factories are remarkably devoid of other cellular membranes, as has long been appreciated from all earlier EM studies (Dales and Simi-

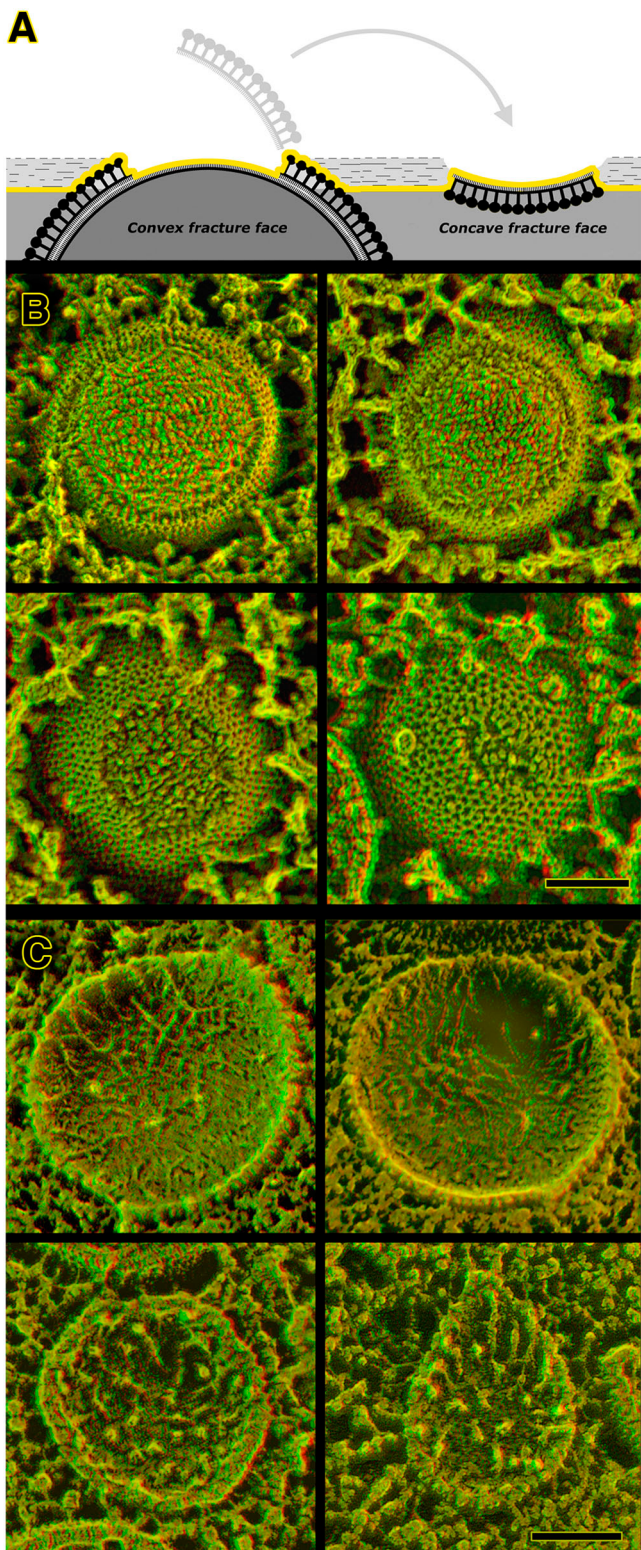


Figure 8. Freeze fracturing of immature vaccinia virions demonstrates that they are composed of only a single lipid membrane. Panel A diagrams how biological membranes split along the center of the bilayer during freeze fracture, yielding two roughly complementary fracture faces. In the case of vaccinia IVs and IMVs, these fracture faces are of course distinctly convex or concave. Deep etching removes a superficial layer of ice (shaded light in the diagram), thereby exposing the immediately adjacent true surfaces of convexly fractured virions. (B) Gallery of IV convex fractures. Regardless of whether they are chemically fixed before freezing or not, IVs display a single fracture face covered with small protuberances

novitch, 1961; Dales, 1963; Dales and Mosbach, 1968; Morgan, 1976).

Deeper cross fractures into IMVs

Bearing importantly on the one membrane/two membrane conundrum being addressed here are the profound structural changes occur in the interior of the IV as it matures. These include a condensation of its core into a dense, relatively “brick”-shaped structure that is surrounded by a ~10-nm-thick “clear zone”. In traditional thin sections, this clear zone is discernable because it is bordered by narrow bands of electron-density (Fig. 4, red highlighting). This has led some investigators to conclude that, in fact, this is the virion’s second “unit membrane”, appearing in a new guise in the IMV (Risco et al., 2002; Sodeik and Krijnse-Locker, 2002). Even the most recent EM tomographic study of vaccinia virions reached this conclusion (Cyrklaff et al., 2005). To explain the mysterious appearing act of this membrane inside the already closed IV envelope, its proponents have had to argue that it was there all the time: namely, as the second membrane of the collapsed cisternae, but that it was so closely opposed to the membrane with the external spikes on IVs that it couldn’t be properly discerned until condensation of viral core drew it inward (Sodeik et al., 1993; Krijnse-Locker et al., 1996; Pedersen et al., 2000; Griffiths, Wepf et al., 2001; Sodeik and Krijnse-Locker, 2002).

If this were so, then we should certainly have been able to demonstrate here a second fracture plane within the IMV (Fig. 9), even though we failed to find any second fracture plane in the IV (Fig. 8). Being now physically separate from the outer envelope of the virus, this putative inner membrane should have been easier to fracture and easier to see. Moreover, we should have expected to see some sort of pattern of intramembrane particles on its fracture faces, if it had existed. This is because several earlier EM studies have shown that the clear zone around the core of IMVs is punctuated by a very distinctive array of “spicules”, which has lead to its having been named the palisade layer (Easterbrook, 1966; Muller and Williamson, 1987; Dubochet et al., 1994). Such a palisade would surely be expected to yield some sort of regular pattern of intramembrane particles on the fracture face of the membrane to which it attached (again, if such a membrane existed).

However, in no case did we obtain any fracture face of this palisade layer; all it ever yielded were cross fractures of the sort shown in Fig. 5 (top). This was true regardless of whether we fractured complete IMVs *in situ* or *in vitro*. Thus, we have no reason to believe that the palisade layer or clear zone of the IMV contains any lipid membrane at all. This fits with the fact

called “intramembrane particles” (which presumably represent transmembrane proteins). Clearly visible on each convex fracture is a step up that marks the transition between the fracture face and the true surface of the IV, where its honeycomb lattice is apparent. (C) Gallery of IV concave fractures. As with the convex fractures above, we have never seen any hint of any jump into what might be a second, closely opposed membrane in the IV envelope. Unlike the convex views, concave fracture faces display only a few intramembrane particles, but mostly randomly oriented fibrils or “stubs” of fibrils, typical of the “plastic distortion” that accompanies freeze fracture even at temperatures below –100°C. Bars, 0.1 μm.

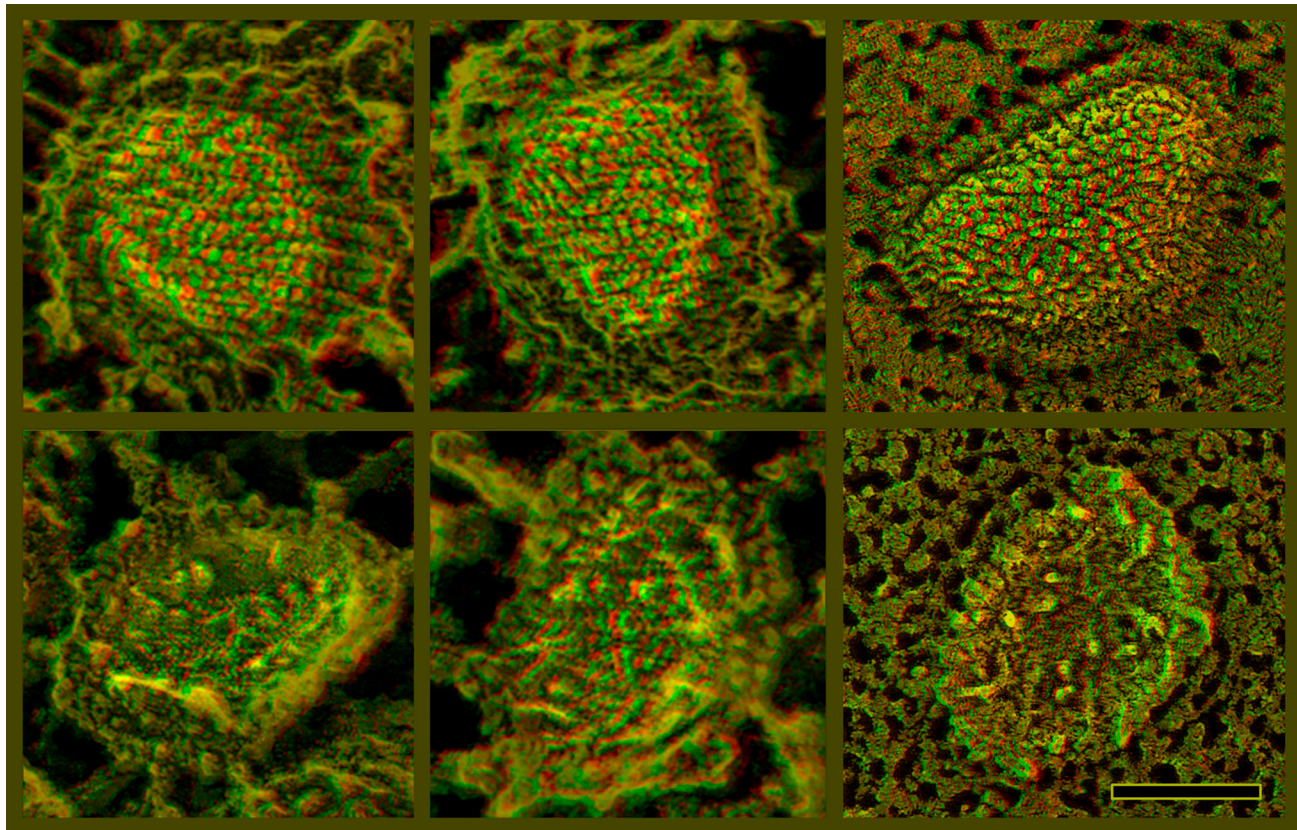


Figure 9. Freeze-fractured IMVs inside infected cells, illustrating that the fracturing properties of IMVs are basically the same as those of IVs in Fig. 8. Convex fractures are above and concave fractures below. Deep etching is to the left and minimal etching is to the right. (Reduced etching has no effect on the appearance of the fracture faces, but obviously eliminates the glimpses of true surface normally seen around the circumferences of convex fractures. Still, these glimpses look just like the surfaces of the whole IMV seen in Fig. 6 A.) Again, IMVs present only one fracture plane in every instance; hence, they too must be surrounded by only one membrane. Bar, 0.1 μ m.

that the appearance of the “membrane” under the palisade layer is unaltered by detergent extraction (Dubochet et al., 1994). Moreover, it fits with our finding that free viral cores delivered into newly infected cells during viral fusion retain their palisade layer and still look like they possess a bilayer when viewed in thin sections, even in freeze-substituted cells; but they still do not freeze fracture as they would if they contained any membrane. Even when thus free in the cytoplasm and no longer surrounded by the IMV envelope, vaccinia cores still invariably cross fracture, and never display any fracture faces (Fig. 5, bottom).

Discussion

The most salient conclusion of this new approach for imaging poxvirus morphogenesis is that at all stages of development, its envelope appears to consist of a single lipid bilayer reinforced on its convex surface by a thick, confluent protein coat. Initially, this coat takes the form of a continuous honeycomb-lattice tightly applied to the convex surface of the virus. During maturation from the IV to the IMV form, this honeycomb coat disappears and is replaced by an even thicker but less obviously regular protein coat. At no time during development does the envelope of the virus appear, or behave during freeze

fracture, as if it possesses a second membrane. Other examples of biological structures that are known to possess double membranes, like mitochondria, plant thylakoids, rod outer segment disks, and even Gram-negative bacteria, invariably display both of their membranes during freeze fracture, because the fracture-plane steps occasionally and randomly between one and the other membrane (Bullivant and Ames, 1966; Clark and Branton, 1968; Fisher and Branton, 1974; Roof and Heuser, 1982; Roof et al., 1982). Likewise, in the most intimately opposed of all membrane arrays, those found in the myelin sheaths of nerves, oblique freeze fractures invariably step through each layer without skipping any, or if they do skip they leave behind double-thick steps (Black et al., 1988; Cullen, 1988; Hasegawa et al., 1988; Rosenbluth, 1988, 1990; Meller, 1990, 1998; Shirasaki and Rosenbluth, 1991; Fujimoto et al., 1996; Maxwell et al., 1999). Not so with vaccinia virus!

Proponents of the two-membrane collapsed-cisternae model of poxvirus formation would thus have to argue that one of the two membranes, and always the same one, refuses to fracture. This would not only be unprecedented for a biological membrane, but would defy two additional observations presented here: namely, (1) that in freeze-substituted material, still only one membrane is visible (Fig. 4); and (2) in none of the

technical approaches used here were any connections of the developing crescents to membrane “loops” or to other closed cellular compartments ever observed (Fig. 3, top left). Instead, developing crescents invariably end abruptly, like old railroad spurs that run off into the grass and stop (Ferlinghetti, 1955).

The only way to explain how such a single railroad track unit membrane could exist free in the cytoplasm is to imagine that it is stabilized by a confluent protein coat, and that is exactly what has been found here. The external spikes long seen on the developing viral crescents and the completed spherical IVs, and long thought to be composed primarily of the protein p65 (D13L; Baldick and Moss, 1987; Miner and Hruby, 1989; Zhang and Moss, 1992; Sodeik et al., 1994; Vanslyke and Hruby, 1994), turn out to be the thin-section representation of a continuous honeycomb lattice, only seeming to be discontinuous and spike-like due to vagaries in the superimposition of its lattice lines in different planes of sectioning and viewing in the EM. Thus, the prescient conclusion of Dales et al. (1978), the first investigators to observe the external spikes on IVs (Stern et al., 1977; Mohandas and Dales, 1995) are entirely justified and explained by the present observations. They concluded that the spike layer stabilized the crescent membrane and imposed a curvature upon it, and they stressed that when the spikes were prevented from associating with the developing IVs by the drug Rifampicin, the IV membrane became floppy and tended to close up upon itself. This latter observation has been confirmed many times, and has been highlighted by many demonstrations of just how promptly crescent formation resumes upon washout of Rifampicin—again, with the crescents invariably displaying the spike layer as soon as they begin to reform (Moss et al., 1969; Grimley et al., 1970; Nagayama et al., 1970; Pennington et al., 1970; Follett and Pennington, 1971; Grimley and Moss, 1971; Moss et al., 1971; Pennington and Follett, 1971). In a subsequent report, we will use the imaging techniques introduced here to confirm that the external lattice is indeed D13L, that D13L is indeed a trimer, and that D13L is indeed capable of polymerizing into a continuous, self-supporting honeycomb (unpublished data).

The observations reported here recapitulate in many ways the history of the discovery of the clathrin lattice around endocytic vesicles (Pearse, 1975; Heuser, 1980). The clathrin coat was first perceived by thin section EM, where transverse cross sections made it look like a set of “peg-like projections” (Roth and Porter, 1964). The occasional glancing section of a coated pit suggested that these projections might be cross-sectional views of a honeycomb lattice (Bowers, 1964). Then DEEM finally provided clear en face views that confirmed it was a honeycomb lattice and confirmed that it curved via the insertion of pentagons (Crick and Watson, 1956; Caspar and Klug, 1962), and that it displayed pentagon/heptagon lattice defects in regions of irregularity (Heuser, 1980). Likewise with the coat on poxviruses, it was first perceived in thin section EM as a set of spike-like projections (Dales, 1963), gave hints in glancing thin sections that it could be a honeycomb (Mohandas and Dales, 1995) and finally has been shown by DEEM to indeed be a complete honeycomb lattice that closely coats the primary envelope of the poxvirus throughout its period of gen-

eration. Moreover, the IV coat displays pentagons in regions of maximal curvature and an abundance of pentagon/heptagon lattice defects in other regions. Fundamental differences between these two lattices include the fact that the clathrin lattice is built of highly extended molecules that contact each other over relatively large distances, thus making a very flexible and open meshwork capable of assuming a wide range of curvature, and of even capable of changing curvature after assembly (Heuser, 1989), whereas the poxvirus coat is presumably built of small globular units (trimers of the 65-kD D13L protein) that form a compact lattice that appears rigid and of fixed curvature, thereby “templating” the constant size of the virion.

Finally, the major conclusion reached in this study, namely that the developing IV envelope is a ragged-edged unitary bilayer membrane, raises the challenge for future research to determine how the building blocks of the IV envelope, many of which are apparently manufactured in the ER, can manage to get transferred to such a freestanding membrane. Among the many different mechanisms that might be envisioned, the following possibilities are worth consideration: (a) piecemeal assembly from side-to-side association of individual proteolipid complexes, which might float around free in the cytoplasm and bind to the inner surface the D13L lattice as it grows; (b) growth from “T”-shaped membrane junctions that viral crescents might form at their free edges with closed cellular compartments like the ER (Fig. 10); or (c) sequestration of viral lipids and coat components in one particular domain of host cell ER, which at some point converts from a closed compartment to an open crescent by the rupture of some opposite, noncoated portion of its surface.

We favor the second possibility because there seems to be an interesting precedent for such a mechanism in the biogenesis of lipid droplets. Lipid droplets are currently thought to be surrounded by monolayers of phospholipids whose hydrophobic acyl chains face inward toward the cores of triglyceride. If so, they are topologically equivalent to single-membrane bilayers lying free in the cytoplasm, but with a lot of extraneous fat trapped between the leaflets of the bilayer (and with no free edges). Current thinking is that lipid droplets form and grow by generating T-junctions with the ER (Fujimoto et al., 1996;

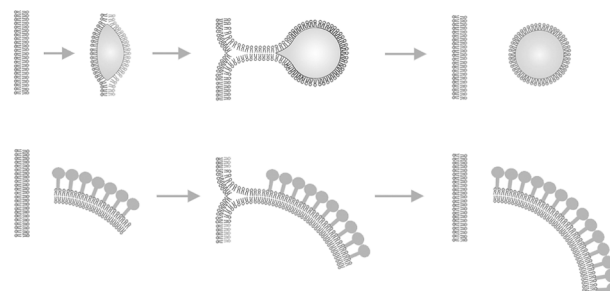


Figure 10. Diagram comparing how lipid droplets are currently thought to form, versus our hypothesis for poxvirus membrane growth. Lipid droplets are thought to form within the membrane of the ER and then bud from it (top). Here, we propose that the crescent-shaped precursors of vaccinia IVs might acquire phospholipids from the ER membrane in a similar manner (bottom). In both cases, an unstable intermediate in the form of a “T-junction” might form transiently, as is thought to occur during all membrane fusion and budding events.

Prates et al., 2000; Brown, 2001; Murphy, 2001; Ostermeyer et al., 2001; Pol et al., 2001; Fukumoto and Fujimoto, 2002; Hope et al., 2002; Caldas and Herman, 2003; Didonato and Braasem, 2003; Ostermeyer et al., 2004). Fig. 10 demonstrates how this is topologically equivalent to mechanism (2) proposed above for vaccinia virus crescent growth. If this equivalency turns out to have any truth to it, then we could further theorize that vaccinia viruses might have coopted or pirated the cellular machinery that normally mediates the transfer of phospholipids and proteins from ER to lipid droplets. Hopefully, future imaging studies using the deep-etch technique (both of poxvirus development and of lipid droplet development) will help to determine whether this idea has any basis in reality.

Materials and methods

Cells and viruses

BS-C-1 or BS-C-40 cells (immortalized African green monkey kidney cells) were grown on small 3×3 mm glass coverslips in DME with Earle's BSS and 10% FCS (HyClone Inc.) and infected with the WR strain of vaccinia virus at a dose of 1–10 pfu/cell for 1 h at 37°C, then maintained in culture overnight in fresh medium. Alternatively, QT6 cells (immortalized Japanese quail fibrosarcoma cells) were grown in Ham's F10 medium plus 10% FCS (HyClone) and infected with the MVA strain of vaccinia virus, then recultured overnight. Thanks to W. Resch and T. Koonina (National Institute of Allergy and Infectious Diseases, Bethesda, MD) for providing some of the vaccinia virus strains used in this study.

Cryopreservation of infected cells

At appropriate times, the MVA-infected QT6 cells on coverslips were briefly rinsed in serum-free, HEPES-buffered Ringer solution (1–5 min) and promptly quick frozen by abrupt application (slamming) of the coverslip onto a liquid helium-cooled copper block with our standard Cryopress (Heuser et al., 1979; Heuser, 1989). This could only be done with MVA, because quick-freezing is likely to preserve virus infectivity, and deep etching can only be done in an open P1 facility. For comparison, WR-infected BSC40 cells on coverslips initially maintained in a P3 facility were chemically fixed with 3% glutaraldehyde in an isotonic HEPES-buffered Ringer solution for 2 h, after which they could be safely transferred to our P1 quick-freeze facility and frozen as above.

Replicating and imaging deep-etched or freeze-dried samples

Coverslips were stored in liquid nitrogen (LN_2) until mounting in a Balzers freeze-etch device (Moor et al., 1961; Moor and Muhlethaler, 1963), where they were warmed to -105°C and immediately freeze fractured (Steere, 1957), then deep etched by letting them sit for 2 min in vacuo (Heuser and Salpeter, 1979), and finally replicated with 2 nm of platinum (Bradley, 1959), which was vacuum evaporated onto them (Zingsheim et al., 1970; Zingsheim, 1972) from 24° above horizontal while they rotated at 20 rpm: standardly termed rotary replication (Fisher and Branton, 1974; Margaritis et al., 1977).

Besides freeze fracture and deep etching, other samples of infected cells or purified virions were glutaraldehyde fixed as above, and then washed scrupulously with many changes of distilled water before quick freezing. This permitted these samples to be totally freeze dried in the Balzers apparatus (by exposure to the vacuum for 15 min at -80°C) before rotary replication as above. This yielded unfractured, undisturbed surface views of cells and virions.

In all cases, replicas were separated from the coverslips by flotation on concentrated hydrofluoric acid, and then washed briefly with 4% sodium hypochlorite (bleach) and several rinses of water, before being retrieved on 400-mesh Formvar-coated grids. These were then viewed with a standard TEM operating at 100 kV and imaged at two different degrees of tilt ($\pm 10^\circ$) with standard EM film. Thereafter, the stereo pairs of film were aligned by superimposition on a copy stand and rerecorded as 4492×3328 pixel (17 Mp) digital images with a digital single-lens reflex camera (Canon EOS-1Ds Mark II). Finally, the digital image pairs were converted, one to red and the other to green, and layered on top of each other with the Screen blending mode in Adobe Photoshop, to create the final 3-D anaglyphs shown here (Heuser, 2000).

Comparison with thin sections of freeze-substituted or cryosectioned material

To obtain images more immediately comparable to earlier electron micrographs of vaccinia viruses, certain quick-frozen cell cultures were worked up for traditional thin sectioning rather than platinum replication. This involved standard freeze substitution at -85°C in dry acetone containing 5% OsO₄ (Feder and Sidman, 1958), followed by embedding in Araldite epoxy resin, which after $+60^\circ\text{C}$ polymerization was thin sectioned at 0.1–0.2- μm thick (to provide added depth), then imaged in 3-D as described above for replicas.

Finally, an additional cross-correlation was provided by generating Tokuyasu-type cryosections of vaccinia virus-infected cells, and then imaging these by DEEM rather than the usual way. This involved first generating standard cryosections of infected cells; e.g., the cells were aldehyde fixed as above, then impregnated with 2M sucrose and frozen slowly by immersion in LN_2 , then cut with a diamond knife at -130°C into 0.1–0.2- μm thick cryosections (Tokuyasu, 1973, 1980, 1984, 1986). To image these slices in replicas rather than as the usual translucent whole mounts, they were picked up on tiny cover glasses rather than on EM grids, then thawed, washed free of sucrose with several changes of water, and finally quick-frozen, freeze dried, and platinum replicated exactly as described for cells and virions above. This yielded remarkably clean cuts through infected cells which looked roughly equivalent to freeze-fractured cells, but which lacked any confusing fracture faces (either because they do not form during sectioning with a diamond knife, or because they do not survive the freeze thawing.)

Abrupt application of viruses to cells by spinoculation

To image viral core structure outside of whole virions, cells were abruptly inoculated with massive amounts of virus (100–500 pfu/cell) by centrifugal inoculation or "spinoculation" (Gordon et al., 1960; Weiss and Dressler, 1960; Osborn and Walker, 1968; Hudson et al., 1976; Tenser, 1978; Smith, 1981; Thiele et al., 1987). This involves centrifuging a suspension of viruses down onto already plated cells, then warming them up to allow viral fusion. To accomplish this, we prepared flat "fillers" for 1.5-ml Eppendorf tubes by filling them halfway with Epoxy resin and polymerizing it at 60°C . Two or three of the tiny 3×3 mm coverslips we use for quick freezing were then arranged on the bottom of the tube, overlaid with a suspension of virions in normal mammalian Ringer's solution, and centrifuged at 3,000 RPM for 4 min in a standard clinical centrifuge equipped with swinging buckets containing special inserts to hold the Eppendorf tubes. The centrifugation was done at room temperature, after which the coverslips were transferred into a warm Ringer's solution at 37°C for 5 min before quick-freezing. This Ringer's solution was mildly acidified because this dramatically enhances poxvirus fusion.

We wish to thank Dr. Bernard Moss for his important intellectual input and guidance throughout this study. We also wish to thank several members of his laboratory at National Institutes of Health, NIAID, including Ms. Andrea Weisberg for providing the excellent Tokuyasu cryosections, Dr. Wolfgang Resch for providing purified VV cores, and Dr. Tania Koonina for providing purified IMVs. We also wish to thank Dr. Suzanne Pontow in Lee Ratner's Lab at Washington University School of Medicine, for performing all the VVR infections for us, under proper P3 conditions. Finally, we wish to thank all the members of our own lab for a superb effort, including Mrs. Robyn Roth for all the EM, Ms. Jennifer Scott for all the computer work, Mrs. Lyussiena Loultcheva for the tissue culturing and light microscopy, and Mr. Dimitar Balgaranov for his engineering and technical support.

This work was supported by United States Public Health Service grant GM29647-22.

Submitted: 30 December 2004

Accepted: 15 March 2005

References

- Baldick, C.J., Jr., and B. Moss. 1987. Resistance of vaccinia virus to rifampicin conferred by a single nucleotide substitution near the predicted NH₂ terminus of a gene encoding an Mr 62,000 polypeptide. *Virology*. 156:138–145.
- Bang, F.B. 1950. Cellular changes in the chick chorio-allantoic membrane infected with herpes simplex and vaccinia; a study with thin sections for the electron microscope. *Bull. Johns Hopkins Hosp.* 87:511–547.
- Bernhard, W., A. Bauer, J. Harrel, and C. Oberling. 1954. Intracytoplasmic forms of the Shope papilloma virus; electron microscopy of ultrafine sections. *Bull. Assoc. Fr. Etud. Cancer*. 41:423–444.

- Black, J.A., R.D. Fields, and S.G. Waxman. 1988. Macromolecular structure of axonal membrane in the optic nerve of the jumpy mouse. *J. Neuropathol. Exp. Neurol.* 47:588–598.
- Bowers, B. 1964. Coated vesicles in the pericardial cells of the aphid. *Protoplasma*. 59:351–367.
- Bradley, D.E. 1959. High-resolution shadow-casting technique for the electron microscope using the simultaneous evaporation of platinum and carbon. *Br. J. Appl. Phys.* 10:198–203.
- Breese, S.S., and C.J. Deboer. 1966. Electron microscope observations of African swine fever virus in tissue culture cells. *Virology*. 28:420–428.
- Brookes, S.M., A.D. Hyatt, T. Wise, and R.M. Parkhouse. 1998. Intracellular virus DNA distribution and the acquisition of the nucleoprotein core during African swine fever virus particle assembly: ultrastructural *in situ* hybridisation and DNase-gold labelling. *Virology*. 249:175–188.
- Brown, D.A. 2001. Lipid droplets: proteins floating on a pool of fat. *Curr. Biol.* 11:R446–R449.
- Buckminster-Fuller, R., and E.J. Applewhite. 1975. Synergetics. MacMillan Publishing Co., New York. 876 pp.
- Bullivant, S., and A. Ames III. 1966. A simple freeze-fracture replication method for electron microscopy. *J. Cell Biol.* 29:435–447.
- Caldas, H., and G.E. Herman. 2003. NSDHL, an enzyme involved in cholesterol biosynthesis, traffics through the Golgi and accumulates on ER membranes and on the surface of lipid droplets. *Hum. Mol. Genet.* 12:2981–2991.
- Caspar, D.L., and A. Klug. 1962. Physical principles in the construction of regular viruses. *Cold Spring Harb. Symp. Quant. Biol.* 27:1–24.
- Clark, A.W., and D. Branton. 1968. Fracture faces in frozen outer segments from the guinea pig retina. *Z. Zellforsch. Mikrosk. Anat.* 91:586–603.
- Cobbold, C., S.M. Brookes, and T. Wileman. 2000. Biochemical requirements of virus wrapping by the endoplasmic reticulum: involvement of ATP and endoplasmic reticulum calcium store during envelopment of African swine fever virus. *J. Virol.* 74:2151–2160.
- Crick, F.H., and J.D. Watson. 1956. Structure of small viruses. *Nature*. 177: 473–475.
- Cullen, M.J. 1988. Freeze-fracture analysis of myelin membrane changes in Wallerian degeneration. *J. Neurocytol.* 17:105–115.
- Cyrklaff, M., C. Risco, J.J. Fernandez, M.V. Jimenez, M. Esteban, W. Baumeister, and J.L. Carrascosa. 2005. Cryo-electron tomography of vaccinia virus. *Proc. Natl. Acad. Sci. USA*. 102:2772–2777.
- Dales, S. 1962. An electron microscope study of the early association between two mammalian viruses and their hosts. *J. Cell Biol.* 13:303–322.
- Dales, S. 1963. The uptake and development of vaccinia virus in strain L cells followed with labeled viral deoxyribonucleic acid. *J. Cell Biol.* 18:51–72.
- Dales, S., V. Milovanovich, B.G. Pogo, S.B. Weintraub, T. Huima, S. Wilton, and G. McFadden. 1978. Biogenesis of vaccinia: isolation of conditional lethal mutants and electron microscopic characterization of their phenotypically expressed defects. *Virology*. 84:403–428.
- Dales, S., and E.H. Mosbach. 1968. Vaccinia as a model for membrane biogenesis. *Virology*. 35:564–583.
- Dales, S., and L. Siminovitch. 1961. The development of vaccinia virus in Earle's L strain cells as examined by electron microscopy. *J. Biophys. Biochem. Cytol.* 10:475–503.
- Didonato, D., and D.L. Brasaeimle. 2003. Fixation methods for the study of lipid droplets by immunofluorescence microscopy. *J. Histochem. Cytochem.* 51:773–780.
- Dubochet, J., M. Adrian, K. Richter, J. Garces, and R. Wittek. 1994. Structure of intracellular mature vaccinia virus observed by cryoelectron microscopy. *J. Virol.* 68:1935–1941.
- Easterbrook, K.B. 1966. Controlled degradation of vaccinia virions *in vitro*: an electron microscopic study. *J. Ultrastruct. Res.* 14:484–496.
- Easterbrook, K.B., and K.R. Rozee. 1971. The intracellular development of vaccinia virus as observed in freeze-etched preparations. *Can. J. Microbiol.* 17:753–757.
- Ericsson, M., B. Sodeik, J.K. Locker, and G. Griffiths. 1997. In vitro reconstitution of an intermediate assembly stage of vaccinia virus. *Virology*. 235:218–227.
- Feder, N., and R.L. Sidman. 1958. Methods and principles of fixation by freeze-substitution. *J. Biophys. Biochem. Cytol.* 4:593–600.
- Ferlinghetti, L. 1955. Just as I used to say. *In Pictures of the Gone World*. San Francisco, The Pocket Poets Series, no. 1. City Lights Publishing, San Francisco. 45.
- Fisher, K., and D. Branton. 1974. Application of the freeze-fracture technique to natural membranes. *Methods Enzymol.* 32:35–44.
- Follett, E.A., and T.H. Pennington. 1971. The mode of action of rifamycins and related compounds on poxvirus. *Adv. Virus Res.* 18:105–142.
- Fujimoto, K., M. Umeda, and T. Fujimoto. 1996. Transmembrane phospho-lipid distribution revealed by freeze-fracture replica labeling. *J. Cell Sci.* 109:2453–2460.
- Fukumoto, S., and T. Fujimoto. 2002. Deformation of lipid droplets in fixed samples. *Histochem. Cell Biol.* 118:423–428.
- Gaylord, W.M., and J.L. Melnick. 1953. Intracellular forms of pox viruses as shown by the electron microscope (vaccinia, ectromelia, Molluscum contagiosum). *J. Exp. Med.* 98:157–297.
- Gordon, F.B., A.L. Quan, and R.W. Trimmer. 1960. Morphologic observations on trachoma virus in cell cultures. *Science*. 131:733–734.
- Griffiths, G., N. Roos, S. Schleich, and J.K. Locker. 2001. Structure and assembly of intracellular mature vaccinia virus: thin-section analyses. *J. Virol.* 75:11056–11070.
- Griffiths, G., R. Wepf, T. Wendt, J.K. Locker, M. Cyrklaff, and N. Roos. 2001. Structure and assembly of intracellular mature vaccinia virus: isolated-particle analysis. *J. Virol.* 75:11034–11055.
- Grimley, P.M., and B. Moss. 1971. Similar effect of rifampin and other rifamycin derivatives on vaccinia virus morphogenesis. *J. Virol.* 8:225–231.
- Grimley, P.M., E.N. Rosenblum, S.J. Mims, and B. Moss. 1970. Interruption by Rifampin of an early stage in vaccinia virus morphogenesis: accumulation of membranes which are precursors of virus envelopes. *J. Virol.* 6:519–533.
- Harford, C.G., E. Rieders, and R. Osborn. 1972. Inhibition of arc-like fragments and immature forms of vaccinia virus by methisazone. *Proc. Soc. Exp. Biol. Med.* 139:558–561.
- Harris, W.J., and J.C. Westwood. 1964. Phosphotungstate staining of vaccinia virus. *J. Gen. Microbiol.* 34:491–495.
- Hasegawa, M., J. Rosenbluth, and J. Ishise. 1988. Nodal and paranodal structural changes in mouse and rat optic nerve during Wallerian degeneration. *Brain Res.* 452:345–357.
- Hasegawa, T., M. Takeuchi, and S. Imamura. 1974. Ultrastructure of molluscum contagiosum virus as revealed by freeze-etching technique. *J. Invest. Dermatol.* 63:331–333.
- Heuser, J. 1980. Three-dimensional visualization of coated vesicle formation in fibroblasts. *J. Cell Biol.* 84:560–583.
- Heuser, J. 1989. Effects of cytoplasmic acidification on clathrin lattice morphology. *J. Cell Biol.* 108:401–411.
- Heuser, J. 2002. Whatever happened to the “microtrabecular concept”? *Biol. Cell.* 94:561–596.
- Heuser, J., and T. Kirchhausen. 1985. Deep-etch views of clathrin assemblies. *J. Ultrastruct. Res.* 92:1–27.
- Heuser, J.E. 2000. Membrane traffic in anaglyph stereo. *Traffic*. 1:35–37.
- Heuser, J.E. 2001. A critical comparison between the two current methods of viewing frozen, live cells in the electron microscope: cryo-electron microscopy versus “deep-etch” electron microscopy. *Biomed. Rev.* 12:11–29.
- Heuser, J.E., and J. Keen. 1988. Deep-etch visualization of proteins involved in clathrin assembly. *J. Cell Biol.* 107:877–886.
- Heuser, J.E., and S.R. Salpeter. 1979. Organization of acetylcholine receptors in quick-frozen, deep-etched, and rotary-replicated Torpedo postsynaptic membrane. *J. Cell Biol.* 82:150–173.
- Heuser, J.E., T.S. Reese, M.J. Dennis, Y. Jan, L. Jan, and L. Evans. 1979. Synaptic vesicle exocytosis captured by quick freezing and correlated with quantal transmitter release. *J. Cell Biol.* 81:275–300.
- Heuser, J.E., J.H. Keen, L.M. Amende, R.E. Lippoldt, and K. Prasad. 1987. Deep-etch visualization of 27S clathrin: a tetrahedral tetraAm. *J. Cell Biol.* 105:1999–2009.
- Hollinshead, M., A. Vanderplasschen, G.L. Smith, and D.J. Vaux. 1999. Vaccinia virus intracellular mature virions contain only one lipid membrane. *J. Virol.* 73:1503–1517.
- Hope, R.G., D.J. Murphy, and J. McLauchlan. 2002. The domains required to direct core proteins of hepatitis C virus and GB virus-B to lipid droplets share common features with plant oleosin proteins. *J. Biol. Chem.* 277:4261–4270.
- Horne, R.W., and P. Wildy. 1963. Virus structure revealed by negative staining. *Adv. Virus Res.* 10:101–170.
- Hudson, J.B., V. Misra, and T.R. Mosmann. 1976. Cytomegalovirus infectivity: analysis of the phenomenon of centrifugal enhancement of infectivity. *Virology*. 72:235–243.
- Hung, T., C. Chou, C. Fang, and Z. Chang. 1980. Morphogenesis of vaccinia virus in the process of envelopment as observed by freeze-etching electron microscopy. *Intervirology*. 14:91–100.
- Husain, M., and B. Moss. 2003. Evidence against an essential role of COPII-mediated cargo transport to the endoplasmic reticulum-Golgi intermediate compartment in the formation of the primary membrane of vaccinia virus. *J. Virol.* 77:11754–11766.

- Ikoma, K., Y. Hiramatsu, F. Uno, M. Yoshida, and S. Nii. 1992. Ultra-high-resolution scanning electron microscopy of vaccinia virus and its recombinant carrying the gag gene of human immunodeficiency virus type 1. *J. Electron Microsc.* (Tokyo), 41:167–173.
- Iyer, L.M., L. Aravind, and E.V. Koonin. 2001. Common origin of four diverse families of large eukaryotic DNA viruses. *J. Virol.* 75:11720–11734.
- Kirchhausen, T., S.C. Harrison, and J. Heuser. 1986. Configuration of clathrin trimers: evidence from electron microscopy. *J. Ultrastruct. Mol. Struct. Res.* 94:199–208.
- Krijnse-Locker, J., S. Schleich, D. Rodriguez, B. Goud, E.J. Snijder, and G. Griffiths. 1996. The role of a 21-kDa viral membrane protein in the assembly of vaccinia virus from the intermediate compartment. *J. Biol. Chem.* 271:14950–14958.
- Margaritis, L.H., A. Elgsaeter, and D. Branton. 1977. Rotary replication for freeze-etching. *J. Cell Biol.* 72:47–56.
- Mathieson, W.B., and P.E. Lee. 1981. Cytology and autoradiography of *Tipula* iridescent virus infection of insect suspension cell cultures. *J. Ultrastruct. Res.* 74:59–68.
- Maxwell, W.L., R. Kosanavit, B.J. McCreath, O. Reid, and D.I. Graham. 1999. Freeze-fracture and cytochemical evidence for structural and functional alteration in the axolemma and myelin sheath of adult guinea pig optic nerve fibers after stretch injury. *J. Neurotrauma.* 16:273–284.
- Medzon, E.L., and H. Bauer. 1970. Structural features of vaccinia virus revealed by negative staining, sectioning, and freeze-etching. *Virology.* 40:860–867.
- Meints, R.H., K. Lee, D.E. Burbank, and J.L. Van Etten. 1984. Infection of a Chlorella-like alga with the virus, PBCV-1: ultrastructural studies. *Virology.* 138:341–346.
- Meints, R.H., K. Lee, and J.L. Van Etten. 1986. Assembly site of the virus PBCV-1 in a Chlorella-like green alga: ultrastructural studies. *Virology.* 154:240–245.
- Meller, K. 1990. Cryo-electron microscopy of vitrified nerve myelin. *Cell Tissue Res.* 262:59–66.
- Meller, K. 1998. Morphology of cryofixed myelin sheath. *Int. Rev. Cytol.* 184: 81–108.
- Melnick, J.L., H. Bunting, W.G. Banfield, M.J. Strauss, and W.H. Gaylord. 1952. Electron microscopy of viruses of human papilloma, molluscum contagiosum, and vaccinia, including observations on the formation of virus within the cell. *Ann. NY Acad. Sci.* 54:1214–1225.
- Miner, J.N., and D.E. Hruby. 1989. Rifampicin prevents virosome localization of L65, an essential vaccinia virus polypeptide. *Virology.* 170:227–237.
- Mitchiner, M.B. 1969. The envelope of vaccinia and orf viruses: an electron-cytochemical investigation. *J. Gen. Virol.* 5:211–220.
- Mohandas, A.R., and S. Dales. 1995. Involvement of spicules in the formation of vaccinia virus envelopes elucidated by a conditional lethal mutant. *Virology.* 214:494–502.
- Moor, H., and K. Muhlethaler. 1963. Fine structure of frozen-etched yeast cells. *J. Cell Biol.* 17:609–628.
- Moor, H., K. Muhlethaler, H. Waldner, and A. Frey-Wyssling. 1961. A new freezing-ultramicrotome. *J. Biophys Biochem Cytol.* 10:1–13.
- Morgan, C. 1976. Vaccinia virus reexamined: development and release. *Virology.* 73:43–58.
- Morgan, C., S.A. Ellison, H.M. Rose, and D.H. Moore. 1954. Structure and development of viruses observed in the electron microscope. *J. Exp. Med.* 100:301–308.
- Morgan, C., S.A. Ellison, H.M. Rose, and D.H. Moore. 1955. Serial sections of vaccinia virus examined at one stage of development in the electron microscope. *Exp. Cell Res.* 9:572–578.
- Moss, B., E.N. Rosenblum, and P.M. Grimley. 1971. Assembly of vaccinia virus particles from polypeptides made in the presence of rifampicin. *Virology.* 45:123–134.
- Moss, B., E.N. Rosenblum, E. Katz, and P.M. Grimley. 1969. Rifampicin: a specific inhibitor of vaccinia virus assembly. *Nature.* 224:1280–1284.
- Muller, G., and J.D. Williamson. 1987. Poxviridae. In *Animal Virus Structure.* M.V. Nermut and A.C. Steven. Elsevier, New York. 421–433.
- Murphy, D.J. 2001. The biogenesis and functions of lipid bodies in animals, plants and microorganisms. *Prog. Lipid Res.* 40:325–438.
- Nagayama, A., B.G. Pogo, and S. Dales. 1970. Biogenesis of vaccinia: separation of early stages from maturation by means of rifampicin. *Virology.* 40:1039–1051.
- Nagington, J., and R.W. Horne. 1962. Morphological studies of orf and vaccinia viruses. *Virology.* 16:248–260.
- Nagington, J., I.M. Lauder, and J.S. Smith. 1967. Bovine papular stomatitis, pseudocowpox and milker's nodules. *Vet. Rec.* 81:306–313.
- Nagington, J., A.A. Newton, and R.W. Horne. 1964. The structure of Orf virus. *Virology.* 23:461–472.
- Nathke, I.S., J. Heuser, A. Lupas, J. Stock, C.W. Turck, and F.M. Brodsky. 1992. Folding and trimerization of clathrin subunits at the triskelion hub. *Cell.* 68:899–910.
- Nermut, M.V. 1972. Negative staining of viruses. *J. Microsc.* 96:351–362.
- Noyes, W.F. 1962a. The surface fine structure of vaccinia virus. *Virology.* 17:282–287.
- Noyes, W.F. 1962b. Further studies on the structure of vaccinia virus. *Virology.* 18:511–516.
- Nunes, J.F., J.D. Vigario, and A.M. Terrinha. 1975. Ultrastructural study of African swine fever virus replication in cultures of swine bone marrow cells. *Arch. Virol.* 49:59–66.
- Osborn, J.E., and D.L. Walker. 1968. Enhancement of infectivity of murine cytomegalovirus in vitro by centrifugal inoculation. *J. Virol.* 2:853–858.
- Ostermeyer, A.G., J.M. Paci, Y. Zeng, D.M. Lublin, S. Munro, and D.A. Brown. 2001. Accumulation of caveolin in the endoplasmic reticulum redirects the protein to lipid storage droplets. *J. Cell Biol.* 152:1071–1078.
- Ostermeyer, A.G., L.T. Ramcharan, Y. Zeng, D.M. Lublin, and D.A. Brown. 2004. Role of the hydrophobic domain in targeting caveolin-1 to lipid droplets. *J. Cell Biol.* 164:69–78.
- Patrizi, G., and J.N. Middelkamp. 1968. Immature forms of vaccinia virus: morphological observations from thin sections of infected human skin. *Virology.* 34:189–192.
- Pearse, B.M.F. 1975. Coated vesicles from pig brain: purification and biochemical characterization. *J. Mol. Biol.* 97:93–98.
- Pedersen, K., E.J. Snijder, S. Schleich, N. Roos, G. Griffiths, and J.K. Locker. 2000. Characterization of vaccinia virus intracellular cores: implications for viral uncoating and core structure. *J. Virol.* 74:3525–3536.
- Pennington, T.H., and E.A. Follett. 1971. Inhibition of poxvirus maturation by rifampicin derivatives and related compounds. *J. Virol.* 7:821–829.
- Pennington, T.H., E.A. Follett, and J.F. Szilagyi. 1970. Events in vaccinia virus-infected cells following the reversal of the antiviral action of rifampicin. *J. Gen. Virol.* 9:225–237.
- Pogo, B.G., and S. Dales. 1969. Two deoxyribonuclease activities within purified vaccinia virus. *Proc. Natl. Acad. Sci. USA.* 63:820–827.
- Pogo, B.G., and S. Dales. 1971. Biogenesis of vaccinia: separation of early stages from maturation by means of hydroxyurea. *Virology.* 43:144–151.
- Pol, A., R. Luetterforst, M. Lindsay, S. Heino, E. Ikonen, and R.G. Parton. 2001. A caveolin dominant negative mutant associates with lipid bodies and induces intracellular cholesterol imbalance. *J. Cell Biol.* 152:1057–1070.
- Prasad, K., J. Heuser, E. Eisenberg, and L. Greene. 1994. Complex formation between clathrin and uncoating ATPase. *J. Biol. Chem.* 269:6931–6939.
- Prattes, S., G. Horl, A. Hammer, A. Blaschitz, W.F. Graier, W. Sattler, R. Zechner, and E. Steyrer. 2000. Intracellular distribution and mobilization of unesterified cholesterol in adipocytes: triglyceride droplets are surrounded by cholesterol-rich ER-like surface layer structures. *J. Cell Sci.* 113:2977–2989.
- Risco, C., J.R. Rodriguez, C. Lopez-Iglesias, J.L. Carrascosa, M. Esteban, and D. Rodriguez. 2002. Endoplasmic reticulum-Golgi intermediate compartment membranes and vimentin filaments participate in vaccinia virus assembly. *J. Virol.* 76:1839–1855.
- Roof, D.J., and J.E. Heuser. 1982. Surfaces of rod photoreceptor disk membranes: integral membrane components. *J. Cell Biol.* 95:487–500.
- Roof, D.J., J.I. Korenbrot, and J.E. Heuser. 1982. Surfaces of rod photoreceptor disk membranes: light-activated enzymes. *J. Cell Biol.* 95:501–509.
- Rosenbluth, J. 1988. Role of glial cells in the differentiation and function of myelinated axons. *Int. J. Dev. Neurosci.* 6:3–24.
- Rosenbluth, J. 1990. Axolemmal abnormalities in myelin mutants. *Ann. NY Acad. Sci.* 605:194–214.
- Roth, T.F., and K.R. Porter. 1964. Yolk protein uptake in the oocyte of the mosquito. *J. Cell Biol.* 20:313–332.
- Salmons, T., A. Kuhn, F. Wylie, S. Schleich, J.R. Rodriguez, D. Rodriguez, M. Esteban, G. Griffiths, and J.K. Locker. 1997. Vaccinia virus membrane proteins p8 and p16 are cotranslationally inserted into the rough endoplasmic reticulum and retained in the intermediate compartment. *J. Virol.* 71:7404–7420.
- Shirasaki, N., and J. Rosenbluth. 1991. Structural abnormalities in freeze-fractured sciatic nerve fibres of diabetic mice. *J. Neurocytol.* 20:573–584.
- Smith, K.M. 1958. A study of the early stages of infection with the *Tipula* iridescent virus. *Parasitology.* 48:459–462.
- Smith, T.F. 1981. Virus. In *Laboratory Procedures in Clinical Microbiology.* J.A. Washington, editor. Springer-Verlag, New York. 195–219, 525–608.
- Sodeik, B., R.W. Doms, M. Ericsson, G. Hiller, C.E. Machamer, W. van't Hof, G. Van Meer, B. Moss, and G. Griffiths. 1993. Assembly of vaccinia virus: role of the intermediate compartment between the endoplasmic

- reticulum and the Golgi stacks. *J. Cell Biol.* 121:521–541.
- Sodeik, B., G. Griffiths, M. Ericsson, B. Moss, and R.W. Doms. 1994. Assembly of vaccinia virus: effects of rifampin on the intracellular distribution of viral protein p65. *J. Virol.* 68:1103–1114.
- Sodeik, B., and J. Krijnse-Locker. 2002. Assembly of vaccinia virus revisited: de novo membrane synthesis or acquisition from the host? *Trends Microbiol.* 10:15–24.
- Spehner, D., S. De Carlo, R. Drillien, F. Weiland, K. Mildner, D. Hanau, and H.J. Rziba. 2004. Appearance of the bona fide spiral tubule of ORF virus is dependent on an intact 10-kilodalton viral protein. *J. Virol.* 78:8085–8093.
- Stasiak, K., S. Renault, M.V. Demattei, Y. Bigot, and B.A. Federici. 2003. Evidence for the evolution of ascoviruses from iridoviruses. *J. Gen. Virol.* 84:2999–3009.
- Steer, C.J., and J.E. Heuser. 1991. Clathrin and coated vesicles: critical determinants of intracellular trafficking. In *Intracellular Trafficking of Proteins*. C.J. Steer and J.A. Hanover, editors. Cambridge, Cambridge University Press. 47–102.
- Steere, R.L. 1957. Electron microscopy of structural detail in frozen biological specimens. *J. Biophys. Biochem. Cytol.* 3:45–60.
- Stern, W., B.G. Pogo, and S. Dales. 1977. Biogenesis of poxviruses: analysis of the morphogenetic sequence using a conditional lethal mutant defective in envelope self-assembly. *Proc. Natl. Acad. Sci. USA*. 74:2162–2166.
- Tenser, R.B. 1978. Ultracentrifugal inoculation of herpes simplex virus. *Infect. Immun.* 21:281–285.
- Thiele, G.M., M.S. Bicak, A. Young, J. Kinsey, R.J. White, and D.T. Purtilo. 1987. Rapid detection of cytomegalovirus by tissue culture, centrifugation, and immunofluorescence with a monoclonal antibody to an early nuclear antigen. *J. Virol. Methods.* 16:327–338.
- Tokuyasu, K.T. 1973. A technique for ultracryotomy of cell suspensions and tissues. *J. Cell Biol.* 57:551–565.
- Tokuyasu, K.T. 1980. Immunochemistry on ultrathin frozen sections. *Histochem. J.* 12:381–403.
- Tokuyasu, K.T. 1984. Immuno-cryoultramicrotomy. In *Immunolabeling for Electron Microscopy*. Elsevier Science Publishers, New York. 71–82.
- Tokuyasu, K.T. 1986. Application of cryoultramicrotomy to immunocytochemistry. *J. Microsc.* 143:139–149.
- Tripler, F., G. Obert, and A. Kirn. 1973. Ultrastructural study of the effect of arginine deprivation on the morphogenesis of vaccinia virus. *J. Ultrastruct. Res.* 42:121–135.
- Van Etten, J.L., M.V. Graves, D.G. Muller, W. Boland, and N. Delaroque. 2002. Phycodnaviridae—large DNA algal viruses. *Arch. Virol.* 147:1479–1516.
- Vanslyke, J.K., and D.E. Hruby. 1994. Immunolocalization of vaccinia virus structural proteins during virion formation. *Virology*. 198:624–635.
- Weiss, E., and H.R. Dressler. 1960. Centrifugation and Rickettsiae and viruses onto cells and its effect on infection. *Proc. Soc. Exp. Biol. Med.* 103:691–695.
- Wyckoff, R.W. 1951. Electron microscopy of chick embryo membrane infected with PR-8 influenza. *Nature*. 168:651–652.
- Wyckoff, R.W. 1953. The electron microscopy of vaccinia-diseased tissues. *Zellforsch. Mikrosk. Anat.* 38:409–420.
- Yule, B.G., and P.E. Lee. 1973. A cytological and immunological study of *Tipula* iridescent virus-infected *Galleria mellonella* larval hemocytes. *Virology*. 51:409–423.
- Zhang, Y., and B. Moss. 1992. Immature viral envelope formation is interrupted at the same stage by lac operator-mediated repression of the vaccinia virus D13L gene and by the drug rifampicin. *Virology*. 187:643–653.
- Zingsheim, H.P. 1972. Membrane structure and electron microscopy. The significance of physical problems and techniques (freeze etching). *Biochim. Biophys. Acta*. 265:339–366.
- Zingsheim, H.P., R. Abermann, and L. Bachmann. 1970. Apparatus for ultrashadowing of freeze etched electron microscopic specimens. *J. Physiol. E: Sci. Instrum.* 3:39–42.